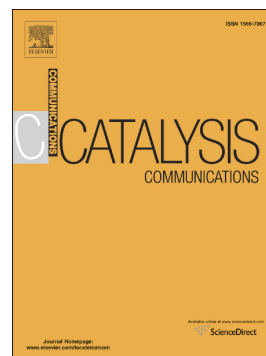


Accepted Manuscript

Photo-deposition preparation of supported Pd catalysts for non-phosgene one-step synthesis of diphenyl carbonate

Changjiang Wu, Xiaojun Yang, Qifeng Tian, Hang Bai, Xiaolu Li



PII: S1566-7367(18)30547-8

DOI: <https://doi.org/10.1016/j.catcom.2018.10.017>

Reference: CATCOM 5528

To appear in: *Catalysis Communications*

Received date: 10 August 2018

Revised date: 3 October 2018

Accepted date: 19 October 2018

Please cite this article as: Changjiang Wu, Xiaojun Yang, Qifeng Tian, Hang Bai, Xiaolu Li, Photo-deposition preparation of supported Pd catalysts for non-phosgene one-step synthesis of diphenyl carbonate. *Catcom* (2018), <https://doi.org/10.1016/j.catcom.2018.10.017>

This is a PDF file of an unedited manuscript that has been accepted for publication. As a service to our customers we are providing this early version of the manuscript. The manuscript will undergo copyediting, typesetting, and review of the resulting proof before it is published in its final form. Please note that during the production process errors may be discovered which could affect the content, and all legal disclaimers that apply to the journal pertain.

Photo-deposition Preparation of Supported Pd Catalysts for Non-phosgene One-step Synthesis of Diphenyl Carbonate

Changjiang Wu^a, Xiaojun Yang^{a, b*}, Qifeng Tian^{a*}, Hang Bai^a, Xiaolu Li^b

(^aKey Laboratory for Green Chemical Process of Ministry of Education, Hubei Key Laboratory of Novel Reactor and Green Chemical Technology, School of Chemical Engineering and Pharmacy, Wuhan Institute of Technology, Wuhan 430205, P. R. China

^bBioproduct Sciences and Engineering Laboratory, Department of Biological Systems Engineering, Washington State University, Richland, WA 99354, USA)

E-mail: 10100201@wit.edu.cn (X. Yang); qftian@wit.edu.cn (Q. Tian)

Abstract

Pd catalysts anchored on manganese oxide octahedral molecular sieves (OMS-2) were synthesized by photo-deposition method, and then used for one-step oxidative carbonylation of phenol to synthesize diphenyl carbonate (DPC). The results showed that the catalytic activity of Pd/OMS-2 catalyst prepared by photo-deposition was apparently better than those prepared by the traditional precipitation and impregnation method, the distribution of Pd particles was more uniform with the average size of 1.3 nm. This may result from the strong interaction between the carriers and the active Pd species. Irradiated for 5 hours at pH 5.0, with the Pd loading of 2.5 wt. %, the highest DPC yield of 18.1% was achieved.

Keywords: Manganese oxide octahedral molecular sieve; photo-deposition; strong metal-support interaction; oxidative carbonylation.

1. Introduction

Diphenyl carbonate (DPC) is an important environmentally benign intermediate, which can be applied to produce pharmaceutical chemicals, pesticides, and polymer materials [1–3]. To date, the main routes for DPC synthesis include phosgene process, transesterification approach, and oxidative carbonylation of phenol. Among them, phosgene process is extremely toxic followed by alkali neutralization of the by-product hydrochloric acid, producing a large amount of waste stream, which makes this process not sustainable and economical [4,5]. Also, the reaction equilibrium constant of the transesterification method is too low to obtain high yield and selectivity [6]. Oxidative carbonylation of phenol direct utilizing phenol, CO and O₂ is an attractive green approach which takes the advantage of low-cost and available raw material with only water as by-product [7]. Considerable contributions have been made to the development of catalytic oxidative carbonylation reactions. The vast majority of these researches focus on an efficient and easily separated supported palladium catalysts [8].

The catalytic performance of supported catalysts is closely related to the particle size of metal loaded on the support [9]. It is generally believed that the catalytic activity of supported catalysts can be improved by decreased size, which is known as “size effect” of the nanoparticles. The activity improvement is caused by highly dispersed nanoclusters with high exposed active sites and maximized metal atom utilization [10–12]. The supported catalysts prepared by the traditional precipitation

method and impregnation method are prone to thermal sintering during the calcination process, resulting in low dispersity and aggregation of the metal particles on support surface. It could make the supported catalysts deactivated or deteriorated [13]. In recent years, photo-deposition method was found to be a fine alternative with low metal loading, high dispersity and stable performance [14]. Aided with photo-assisted redox reaction, the decomposition of metal precursor occurred and atomically dispersed catalysts were obtained [13]. According to Zheng's research [15], ethylene glycol (EG) radical could be released on the TiO_2 surface under mild UV conditions, then a highly stable, atomically dispersed Pd catalyst was anchored on TiO_2 nanosheets through a unique "PdCl₂-EG radical- TiO_2 " interface. The catalyst shows a very high catalytic activity in hydrogenation of C=C and C=O. In theory, the utmost distribution of supported metal catalysts is monoatomic dispersity [16]. Therefore, photochemical technology provides us with a tactic to obtain high-performance supported catalysts [17–20].

A new type of molecular sieves, manganese oxides octahedral molecular sieves (OMS-2), has been extensively investigated in catalysis, gas cleansing, separation, batteries, and chemical sensing. OMS-2 can also be used as photocatalysts due to the property of semiconductor [21]. Liu et al. studied the solid-phase photocatalytic degradation of polyethylene film with OMS-2 in the ambient air under ultraviolet and visible light irradiation [22]. Iyer et al. found that K-OMS-2 prepared by solvent-free method showed the highest activity for selective oxidation of 2-propanol to acetone under visible light irradiation [23]. Based on the photocatalysis performance of

OMS-2, we aimed to prepare palladium supported catalysts on OMS-2 by photo-deposition method. This method may afford high performance catalysts with small sizes and high dispersity. The palladium catalysts with smaller particle size and higher dispersity prevented the reduction and sintering of the active species [24,25]. Therefore, we prepared palladium supported catalysts by photo-deposition method, and the properties and catalytic performance were evaluated in the oxidative carbonylation reaction compared with that prepared by the traditional precipitation and impregnation method.

2. Experimental

2.1 Catalysts Preparation

The manganese oxide octahedral molecular sieves (OMS-2) was prepared by a conventional reflux method [26,27]. The supported Pd/OMS-2 catalysts were prepared by photo-deposition (PD) (Figure S1), precipitation (Pre) and impregnation (IM) methods. The palladium precursor solution was obtained by dissolving the solid PdCl₂ (1.68 g) in 200.0 ml deionized water with the pH being adjusted to 2.0 with concentrated hydrochloric acid. Please see the Supplementary Materials for additional details.

2.2 Catalysts activity evaluation

The oxidative carbonylation reaction was performed in a 250.0 ml stainless steel autoclave equipped with a magnetic stirrer. Phenol (50.0 g), tetrabutylammonium

bromide (TBAB, 1.0 g) for stabilizing the Pd nanoparticles [28]) and the as-prepared catalyst (1.0 g) were introduced into the autoclave. Then the autoclave was sealed and heated to 65 °C. Subsequently, the reaction was carried at a pressure of 5.0 MPa and the gas mixture of CO and O₂ (CO/O₂ = 47/3 molar ratio) was charged. The reaction was allowed to proceed for 4 hours as a cycle. Then, the autoclave was cooled down and the products were collected. The yields of final products were determined by a capillary gas chromatography instrument (GC-8000, China) with a FID detector and a SE-54 capillary column. The activity tests were carried out under a kinetic regime without the impact of mass transfer limitations.

2.3 Catalysts Characterization

The X-ray diffraction (XRD) patterns were recorded on a BRUKER D8 ADVANCE X-ray diffractometer with Cu K_α radiation source. The 2θ scanning range was from 20° to 80°, and the operating voltage and current were set as 40 kV and 40 mA, respectively. Transmission electron microscope (TEM) images were obtained with a JEOLJEM-2100 instrument at an acceleration voltage of 200 kV. X-ray photoelectron spectroscopy (XPS) was carried out on a VG Multilab 2000 using Al K_α radiation. The spectra were corrected by referencing the C1s peak at 284.8 eV. H₂ temperature-programmed reduction (H₂-TPR) profiles of the samples (ca. 100 mg) were obtained on an AutoChem II 2920 Chemisorption Analyzer. The H₂-TPR profile of each sample was recorded during the reduction process at ramp of 10 °C/min from room temperature to 500 °C in a mixture of 5% H₂+ 95% A_r (25 mL / min).

3. Results and discussion

3.1 Characterization of catalysts

Figure 1 showed the XRD patterns of three catalysts. Diffraction peaks of all samples at $2\theta=28.9^\circ$, 37.5° , 42.1° and 50.0° were consistent with the standard diffraction peaks of OMS-2(JCPDS 29-1020), indicating that all the as-prepared catalysts retained the same crystal structure. After Pd loaded, the crystal structure of OMS-2 did not change. However, no diffraction peak of palladium species appeared, which suggested that Pd particles were highly dispersed on OMS-2 supports. It was reported that characteristic diffraction peaks in XRD pattern cannot be observed when the average particles size is smaller than 4.0 nm [29]. In addition, the 2.5 wt. % loading of Pd is relatively low, so we speculate that Pd is well dispersed on the surface of OMS-2 supports with small particle size.

TEM images in Figure 2 demonstrate the particle distribution of active palladium species. It could be seen that the particle size of Pd prepared by photo-deposition method is very small and well distributed even if being calcined. However, the Pd nanoparticles prepared by precipitation and impregnation method were severely agglomerated in Figure S2. Nagai's reported that the sintering inhibition effect on Pt can be controlled by the electron density of oxygen in the support through the Pt-oxide-support interaction [30], even if being calcined. Here, we used ethylene glycol radicals and Pd to form complexes and to enhance the interaction between Pd species and OMS-2. Moreover, the dispersity of Pd particles was yet well with the

mass ratio of Pd loading increasing from 2.5 wt. % to 5.0 wt. %, although Pd particle sizes increased from 1.3 nm to 3.5 nm.

The catalysts were further characterized by H₂-TPR to analyze the interaction between Pd species and OMS-2 supports, and the spectra are displayed in Figure 3. For each sample, there was only one wide reduction peak can be observed at below 400°C. The presence of wide plateaus in the spectra indicates multiple reduction peaks overlap together [25,31]. Zhang [32] had reported that the hydrogen reduction peaks of Pd/OMS-2 catalyst at 100°C~200°C involved one reduction peak of PdO to metallic Pd⁰. Compared to Pd/OMS-2-Pre and Pd/OMS-2-IM catalysts, onset temperature of reduction peak for Pd/OMS-2-PD catalyst is the lowest at 58 °C, indicating the strongest redox ability at low temperature. The spectra also revealed that the reducing properties of Pd species are strongly affected by the preparation methods. The Pd/OMS-2-PD catalysts possess much stronger metal-support interaction than the other two, which resulted in more highly dispersed Pd species and better catalytic performance in the oxidative carbonylation of phenol.

To obtain detailed information on surface compositions and chemical state of each element for all samples, the XPS analysis was conducted. The Pd 3d XPS spectra of the samples are shown in Figure 4, and their quantitative analysis results are summarized in Table S1. As shown in Figure 4, Pd⁰ is absent from all samples, because the binding energy of all peaks shifts toward a higher binding energy at 337.2eV related to Pd 3d_{5/2}. This phenomenon shows that there is no fitting peak for Pd⁰ after the peak separation. The binding energy and the half peak width of Pd 3d_{5/2}

are negatively correlated to the size of the Pd nanoparticles, so it can be inferred that the Pd nanoparticles in the catalyst have extremely small size and are dispersed on the surface of the support. Compared to the Pd/OMS-2-Pre and Pd/OMS-2-IM catalysts, the Pd 3d binding energy of the Pd/OMS-2-PD catalyst is the highest, suggesting the size of the Pd nanoparticles is the smallest. This conclusion is consistent with the TEM results. The content of Pd⁴⁺ in Pd/OMS-2-PD-before calcined and Pd/OMS-2-PD is higher than Pd/OMS-2-Pre and Pd/OMS-2-IM. It suggests the valence state of palladium species for Pd/OMS-2-PD samples remains bivalence or higher before and after calcination. During the photo-deposition process, the presence of palladium oxides is commonly ascribed to the surface oxidation of nanoparticulate by prolonged extensive exposure to air. Moreover, these nanoparticles prepared by the photo-deposition method are easily oxidized at a low temperature due to small size of Pd nanoparticles, which results in a transfer from Pd⁰ to active Pd²⁺. It can be expected that the Pd/OMS-2-PD catalyst may have better catalytic activity than the Pd/OMS-2-Pre and Pd/OMS-2-IM catalysts.

As shown in Figure 5, O1s XPS spectra of the samples could be deconvoluted into two peaks of oxygen species: one lattice oxygen (O_α) peak bonded to metal cations in a coordinatively saturated environment assigned at 529.7 eV, and another surface adsorbed oxygen (O_β) peak bonded to metal cations in a low-coordination environment positioned at 531.3 eV [33]. As seen from Table S2, the Pd/OMS-2-PD sample possesses the highest O_β/O_α atomic ratio. Furthermore, the increased oxygen vacancies is conducive to the migration of surface oxygen species, so the rate of

oxygen species migration on the surface of Pd/OMS-2-PD catalyst is the fastest among the three catalysts.

3.2 Catalytic performance in oxidative carbonylation of phenol

Figure 6 shows the catalytic activity of supported Pd catalyst prepared by three methods in oxidative carbonylation of phenol. The results showed that the catalytic activity of Pd/OMS-2-PD was better than that of Pd/OMS-2-Pre and Pd/OMS-2-IM under the same conditions with a longer catalyst life and no significant loss of catalytic activity after 24 h, and the stability of Pd/OMS-2-PD catalyst was also proved by the cycle experiments (Table S3). The DPC yield reached 20.4% at 24h. Whereas, the catalyst prepared by precipitation method and impregnation method was inactive after 20 h. The deactivation cause maybe ascribed to Pd leaching, which has been discussed in our previous study [25]. The DPC yield (using Pd/OMS-2-Pre catalysts) remained 15.5%. The order of the catalytic activity was: Pd/OMS-2-PD > Pd/OMS-2-Pre > Pd/OMS-2-IM. For three kinds of catalysts prepared, the selectivity are all above 95.0 % (Table S4).

The activity data illustrated that Pd/OMS-2-PD has a significantly higher activity, probably related to the preparation process. For the catalyst prepared by photo-deposition, the ethylene glycol in the solution becomes ethylene glycol radicals after irradiation. Cl⁻ of PdCl₄²⁻ is gradually replaced by ethylene glycol radicals to form a complex [PdCl_{4-x}(EG)_x]^{-2+x}. Then the coordinated ethylene glycol gradually

transforms Pd^{2+} into metallic Pd. A part of the ethylene glycol and Pd continues to coordinate, so that the Pd particles are consolidated and the aggregation can be inhibited. The resultant Pd nanoparticles are eventually oxidized to PdO. The reaction mechanism is shown in Figure S3. When calcinated at high temperature, the Pd particle size of the Pd/OMS-2-PD catalyst remains almost the same as that uncalcined. While the Pd particles of Pd/OMS-2-Pre and Pd/OMS-2-IM samples are easily aggregated without consolidation with EG radical. The corresponding aggregation was observed in Figure 2.

Numerous studies have shown that the pH value of the precursor solution is a crucial factor influencing the catalytic performance of the Pd catalyst. Considering that the isoelectric point (IEP) of OMS-2 is about 6.2 [34], the net charge of OMS-2 surface at pH <6.0 can be positive and can absorb anion. PdCl_4^{2-} can be combined with OMS-2 through electrostatic attraction. However, the electrostatic force between the support and PdCl_4^{2-} is relatively low, so Pd species are easy to sinter or fall off after calcination. Table S5 shows the effects of pH value on catalytic activity during preparation. There is no significant disagreement on DPC yield with varied pH value, suggesting that it is limited for electrostatic force to immobilize Pd species, which further explains the importance of EG radical in photo-deposition method.

Besides, the performance of the catalysts of Pd/OMS-2-PD prepared with different Pd loadings was studied. As shown in Table S5, the reaction rate rises with the increase of Pd loading from 0.5 wt. % to 2.5 wt. %. We propose that the strength of the Mn-O bond is weakened due to the strong interaction between ethylene glycol

and the support, which favors the adsorption and activation of CO and phenol by active Pd²⁺ sites on the manganese oxide [35]. Therefore, the catalytic activity is enhanced. However, the high Pd loading causes the aggregation of Pd noble metals into larger particles, and then the catalytic activity is reduced.

4. Conclusion

Compared with traditional precipitation method and impregnation method, photo-deposition method can be used to prepare small-size, high dispersity, and long-life catalyst. The excellent properties were confirmed by TEM images, H₂-TPR analysis and activity test data. The particle size of catalysts prepared by the photo-deposition method is 1.3 nm. The excellent performance is related to the coordination of ethylene glycol radicals and PdCl₄²⁻, which facilitates the consolidation and homogenous dispersion of small-size Pd particles. There is no significant loss of catalytic activity after 24 hours, and the DPC yield was up to 20.4% at 24 hours.

Acknowledgements

We are grateful for the financial support from Hubei Provincial Natural Science Foundation of China (Grant No.2016CFA079) and the Graduate Innovative Funds of Wuhan Institute of Technology (No.CX2017132).

References

- [1] J. Gong, X. Ma, S. Wang, Phosgene-free approaches to catalytic synthesis of diphenyl carbonate and its intermediates, *Applied Catalysis A: General*. 316 (2007) 1–21. doi:10.1016/j.apcata.2006.09.006.
- [2] J.L. Spivack, J.N. Cawse, D.W. Whisenhunt, B.F. Johnson, K. V. Shalyaev, J. Male, E.J. Pressman, J.Y. Ofori, G.L. Soloveichik, B.P. Patel, T.L. Chuck, D.J. Smith, T.M. Jordan, M.R. Brennan, R.J. Kilmer, E.D. Williams, Combinatorial discovery of metal co-catalysts for the carbonylation of phenol, *Applied Catalysis A: General*. 254 (2003) 5–25. doi:10.1016/S0926-860X(03)00259-X.
- [3] J. Lee, C. Song, J. Kim, J. Kim, Preparation of aromatic polycarbonate nanoparticles using supercritical carbon dioxide *, *Journal of Nanoparticle Research*. (2002) 53–59. doi- 10.1023/a:1020107522135.
- [4] W.B. Kim, U.A. Joshi, J.S. Lee, Making Polycarbonates without Employing Phosgene: An Overview on Catalytic Chemistry of Intermediate and Precursor Syntheses for Polycarbonate, *Industrial & Engineering Chemistry Research*. 43 (2004) 1897–1914. doi:10.1021/ie034004z.
- [5] S. Fukuoka, M. Tojo, H. Hachiya, M. Aminaka, K. Hasegawa, Green and Sustainable Chemistry in Practice: Development and Industrialization of a Novel Process for Polycarbonate Production from CO₂ without Using Phosgene, *Polymer Journal*. 39 (2007) 91–114. doi:10.1295/polymj.PJ2006140.

- [6] Y. Ono, Dimethyl carbonate for environmentally benign reactions, *Pure and Applied Chemistry*. 68 (1996) 367–375. doi:10.1351/pac199668020367.
- [7] H. Ishii, M. Ueda, K. Takeuchi, M. Asai, Oxidative carbonylation of phenol to diphenyl carbonate catalyzed by bis(benzonitrile)dichloropalladium in the presence of polyvinylpyrrolidone, *Catalysis Communications*. 2 (2001) 17–22. doi:10.1016/S1566-7367(01)00002-4.
- [8] X.F. Wu, H. Neumann, M. Beller, Palladium-catalyzed oxidative carbonylation reactions, *ChemSusChem*. 6 (2013) 229–241. doi:10.1002/cssc.201200683.
- [9] Y. Lei, F. Mehmood, S. Lee, J. Greeley, B. Lee, S. Seifert, R.E. Winans, J.W. Elam, R.J. Meyer, P.C. Redfern, D. Teschner, R. Schlogl, M.J. Pellin, L.A. Curtiss, S. Vajda, Increased Silver Activity for Direct Propylene Epoxidation via Subnanometer Size Effects, *Science*. 328 (2010) 224–228. doi:10.1126/science.1185200.
- [10] M. Haruta, T. Kobayashi, H. Sano, N. Yamada, Novel Gold Catalysts for the Oxidation of Carbon Monoxide at a Temperature far Below 0 °C, *Chemistry Letters*. 16 (1987) 405–408. doi:10.1246/cl.1987.405.
- [11] M. Valden, Onset of Catalytic Activity of Gold Clusters on Titania with the Appearance of Nonmetallic Properties, *Science*. 281 (1998) 1647–1650. doi:10.1126/science.281.5383.1647.
- [12] H.-G. Boyen, Oxidation-Resistant Gold-55 Clusters, *Science*. 297 (2002) 1533–1536. doi:10.1126/science.1076248.
- [13] Z. Zhu, Z. Lu, D. Wang, X. Tang, Y. Yan, W. Shi, Y. Wang, N. Gao, X. Yao,

- H. Dong, Construction of high-dispersed Ag/Fe₃O₄/g-C₃N₄ photocatalyst by selective photo-deposition and improved photocatalytic activity, *Applied Catalysis B: Environmental*. 182 (2016) 115–122. doi:10.1016/j.apcatb.2015.09.029.
- [14] D.J. Ehrlich, R.M.O. Jr, T.F. Deutsch, Photodeposition of metal films with ultraviolet laser light, 23 (1986). doi:10.1116/1.571724.
- [15] P. Liu, Y. Zhao, R. Qin, S. Mo, G. Chen, L. Gu, D.M. Chevrier, P. Zhang, Q. Guo, D. Zang, B. Wu, Photochemical route for synthesizing atomically dispersed palladium catalysts, (2016) 1–6. doi:10.1126.
- [16] S. Lee, B. Lee, F. Mehmood, S. Seifert, J.A. Libera, J.W. Elam, J. Greeley, P. Zapol, L.A. Curtiss, M.J. Pellin, P.C. Stair, R.E. Winans, S. Vajda, Oxidative decomposition of methanol on subnanometer palladium clusters: The effect of catalyst size and support composition, *Journal of Physical Chemistry C*. 114 (2010) 10342–10348. doi:10.1021/jp912220w.
- [17] J. Chen, J.C. Lin, V. Purohit, M.B. Cutlip, S.L. Suib, Photoassisted catalytic oxidation of alcohols and halogenated hydrocarbons with amorphous manganese oxides, *Catalysis Today*. 33 (1997) 205–214. doi:10.1016/S0920-5861(96)00119-8.
- [18] Q. Zhang, X. Cheng, C. Zheng, X. Feng, G. Qiu, W. Tan, F. Liu, Roles of manganese oxides in degradation of phenol under UV-Vis irradiation: Adsorption, oxidation, and photocatalysis, *Journal OF Environmental Sciences*. 23 (2011) 1904–1910. doi:10.1016/S1001-0742(10)60655-9.

- [19] A. Ibadon, P. Fitzpatrick, Heterogeneous Photocatalysis: Recent Advances and Applications, *Catalysts*. 3 (2013) 189–218. doi:10.3390/catal3010189.
- [20] A. Winnerl, R.N. Pereira, M. Stutzmann, Photo-induced changes of the surface band bending in GaN: Influence of growth technique, doping and polarity, *Journal of Applied Physics*. 121 (2017). doi:10.1063/1.4983846.
- [21] S.A. Alzahrani, S.A. Al-Thabaiti, W.S. Al-Arjan, M.A. Malik, Z. Khan, Preparation of ultra long α -MnO₂ and Ag@MnO₂ nanoparticles by seedless approach and their photocatalytic performance, *Journal of Molecular Structure*. 1137 (2017) 495–505. doi:10.1016/j.molstruc.2017.02.068.
- [22] G. Liu, S. Liao, D. Zhu, J. Cui, W. Zhou, Solid-phase photocatalytic degradation of polyethylene film with manganese oxide OMS-2, *Solid State Sciences*. 13 (2011) 88–94. doi:10.1016/j.solidstatesciences.2010.10.014.
- [23] A. Iyer, H. Galindo, S. Sithambaram, C. King'ondeu, C.H. Chen, S.L. Suib, Nanoscale manganese oxide octahedral molecular sieves (OMS-2) as efficient photocatalysts in 2-propanol oxidation, *Applied Catalysis A: General*. 375 (2010) 295–302. doi:10.1016/j.apcata.2010.01.012.
- [24] Y. Hu, X. Yang, S. Cao, J. Zhou, Y. Wu, J. Han, Z. Yan, M. Zheng, Effect of the dispersants on Pd species and catalytic activity of supported palladium catalyst, *Applied Surface Science*. 400 (2017) 148–153. doi:10.1016/j.apsusc.2016.12.182.
- [25] C. Yin, J. Zhou, Q. Chen, J. Han, Y. Wu, X. Yang, Deactivation causes of supported palladium catalysts for the oxidative carbonylation of phenol,

- Journal of Molecular Catalysis A: Chemical. 424 (2016) 377–383.
doi:10.1016/j.molcata.2016.07.028.
- [26] R.N. DeGuzman, Y.F. Shen, E.J. Neth, S.L. Suib, C.L. O'Young, S. Levine, J.M. Newsam, Synthesis and Characterization of Octahedral Molecular Sieves (OMS-2) Having the Hollandite Structure, *Chemistry of Materials*. 6 (1994) 815–821. doi:10.1021/cm00042a019.
- [27] X. Chen, Y.F. Shen, S.L. Suib, C.L. O'Young, Characterization of manganese oxide octahedral molecular sieve (M-OMS-2) materials with different metal cation dopants, *Chemistry of Materials*. 14 (2002) 940–948. doi:10.1021/cm000868o.
- [28] L. Ronchin, A. Vavasori, E. Amadio, G. Cavinato, L. Toniolo, Oxidative carbonylation of phenols catalyzed by homogeneous and heterogeneous Pd precursors, *Journal of Molecular Catalysis A: Chemical*. 298 (2009) 23–30. doi:10.1016/j.molcata.2008.09.028.
- [29] K.A.M. Ahmed, H. Peng, K. Wu, K. Huang, Hydrothermal preparation of nanostructured manganese oxides (MnO_x) and their electrochemical and photocatalytic properties, *Chemical Engineering Journal*. 172 (2011) 531–539. doi:10.1016/j.cej.2011.05.070.
- [30] Y. Nagai, T. Hirabayashi, K. Dohmae, N. Takagi, T. Minami, H. Shinjoh, S. Matsumoto, Sintering inhibition mechanism of platinum supported on ceria-based oxide and Pt-oxide-support interaction, *Journal of Catalysis*. 242 (2006) 103–109. doi:10.1016/j.jcat.2006.06.002.

- [31] F. Wang, H. Dai, J. Deng, G. Bai, K. Ji, Y. Liu, Manganese oxides with rod-, wire-, tube-, and flower-like morphologies: Highly effective catalysts for the removal of toluene, *Environmental Science and Technology*. 46 (2012) 4034–4041. doi:10.1021/es204038j.
- [32] Q. Zhang, Q. Liu, P. Ning, X. Liu, L. Xu, Z. Song, Y. Duan, T. Zhang, Performance and kinetic study on Pd/OMS-2 catalyst for CO catalytic oxidation: effect of preparation method, *Research on Chemical Intermediates*. 43 (2017) 2017–2032. doi:10.1007/s11164-016-2743-0.
- [33] Z. Fu, L. Liu, Y. Song, Q. Ye, S. Cheng, T. Kang, H. Dai, Catalytic oxidation of carbon monoxide, toluene, and ethyl acetate over the xPd/OMS-2 catalysts: Effect of Pd loading, *Frontiers of Chemical Science and Engineering*. 11 (2017) 185–196. doi:10.1007/s11705-017-1631-5.
- [34] W. Xiao, H. Xia, J.Y.H. Fuh, L. Lu, Growth of single-crystal α -MnO₂ nanotubes prepared by a hydrothermal route and their electrochemical properties, *Journal of Power Sources*. 193 (2009) 935–938. doi:10.1016/j.jpowsour.2009.03.073.
- [35] W. Gao, The influence of silver on the structural, redox and catalytic properties of the cryptomelane-type manganese oxides in the low-temperature CO oxidation reaction, *Applied Catalysis B: Environmental*. 75 (2007) 107–117. doi:10.1016/j.apcatb.2007.04.002.

Figures and scheme Captions

Figure 1. XRD patterns of Pd/OMS-2 by different methods: Pd/OMS-2-PD, Pd/OMS-2-Pre, and Pd/OMS-2-IM

Figure 2. TEM images of (a) Pd/OMS-2-PD with 2.5wt% loading and (b) Pd/OMS-2-PD with 5wt % loading, and distribution histograms of the Pd particles in Pd/OMS-2-PD with 2.5wt% loading and Pd/OMS-2-PD with 5wt % loading

Figure 3. H₂-TPR profiles of the catalysts prepared by different methods: Pd/OMS-2-PD, Pd/OMS-2-Pre and Pd/OMS-2-IM

Figure 4. Pd 3d spectra of Pd/OMS-2-PD-before calcined, Pd/OMS-2-PD, Pd/OMS-2-Pre and Pd/OMS-2-IM

Figure 5. O 1s spectra of Pd/OMS-2-PD-before calcined, Pd/OMS-2-PD, Pd/OMS-2-Pre, and Pd/OMS-2-IM

Figure 6. Catalytic activity of different catalysts: Pd/OMS-2-PD, Pd/OMS-2-Pre, and Pd/OMS-2-IM

Highlights

- Photo-deposition can prepare high dispersity, small-size and long-life catalyst.
- The Pd particles were homogenously dispersed and consolidated on the OMS-2.
- The yield of DPC can reach 18.1% by using the catalyst of photo-deposition method.

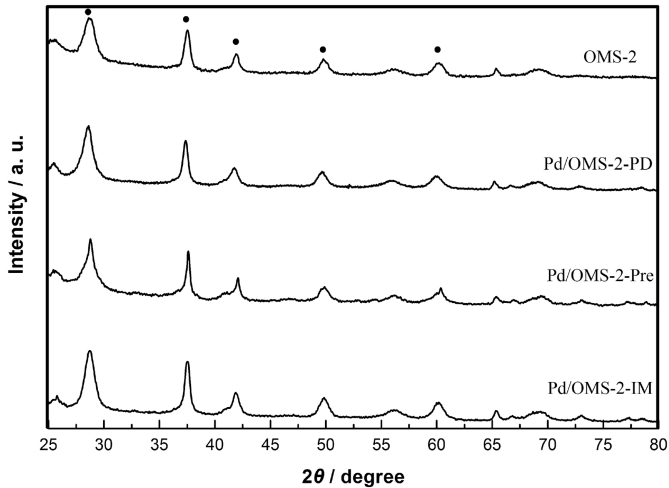


Figure 1

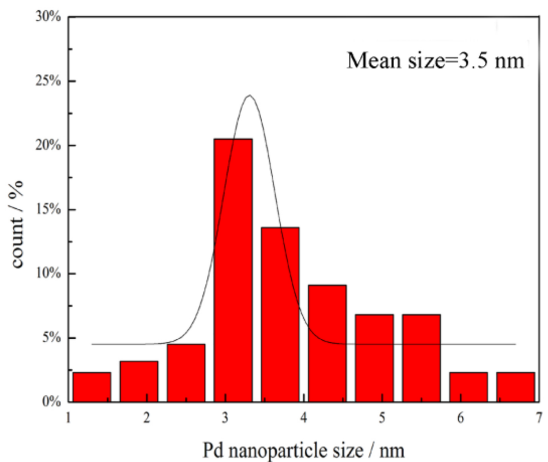
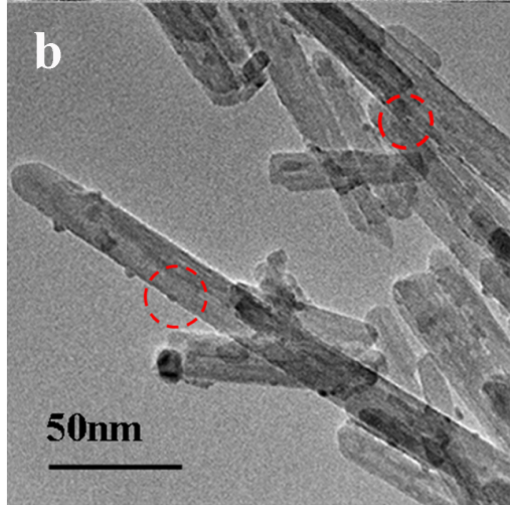
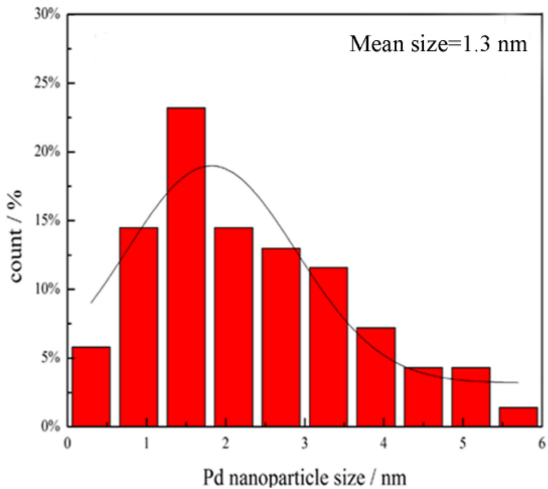
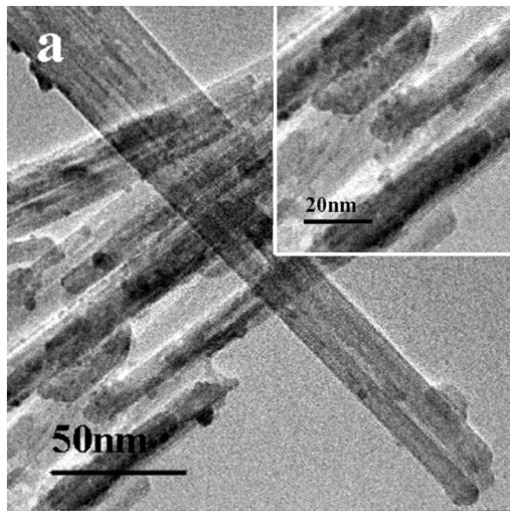


Figure 2

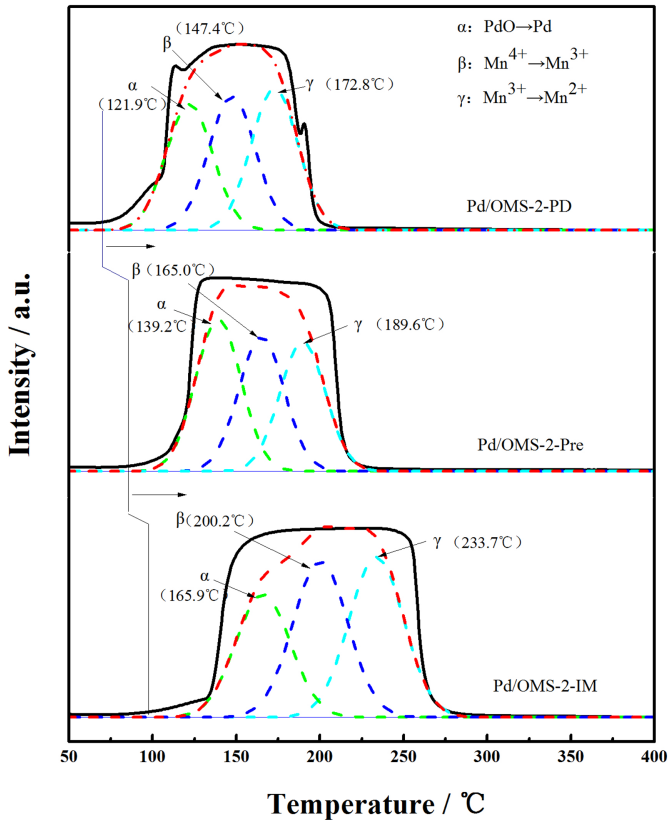


Figure 3

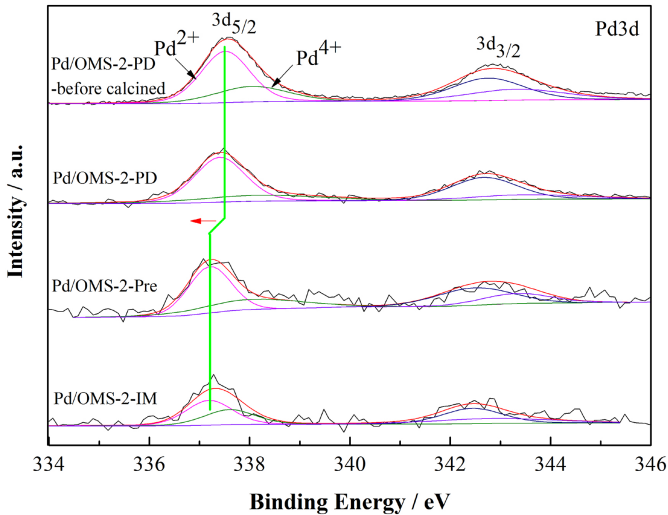


Figure 4

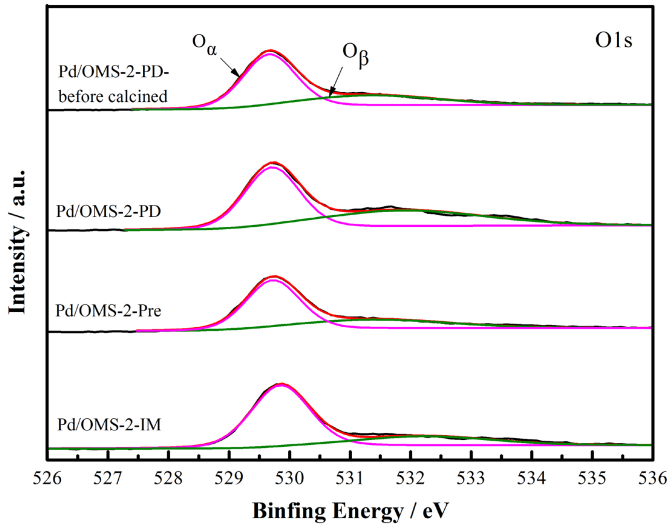


Figure 5

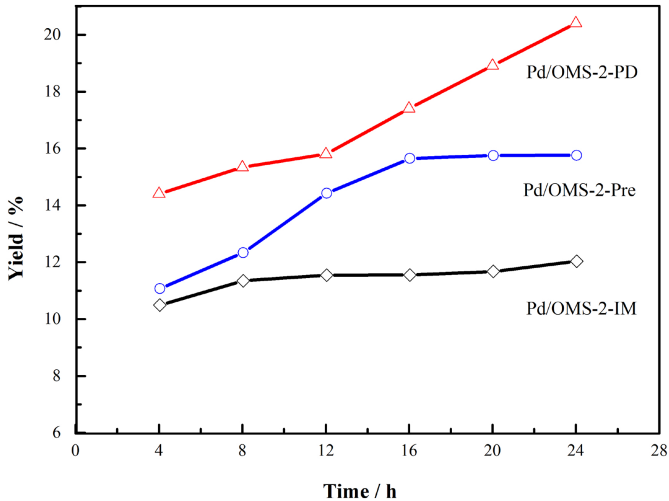


Figure 6